

Room-temperature Transport Properties of High Drift Mobility Two-dimensional Electron Gas Confined in a Strained Si Quantum Well

Maksym Myronov, Kentarou Sawano, Kohei M. Itoh¹, and Yasuhiro Shiraki

Advanced Research Laboratories, Musashi Institute of Technology, 8-15-1 Todoroki, Setagaya-ku, Tokyo158-0082, Japan

¹Department of Applied Physics and Physico-Informatics, Keio University, Yokohama 223-8522, Japan

Received December 1, 2007; accepted December 18, 2007; published online January 25, 2008

The drift mobility, carrier density and conductivity of the two-dimensional electron gas (2DEG) confined in the tensilely strained 15 nm Si quantum well (QW) of SiGe heterostructures were obtained by mobility spectrum analysis at room-temperature. The highest 2DEG drift mobility of $2900 \text{ cm}^2 \text{ V}^{-1} \text{ s}^{-1}$ with carrier density of $1 \times 10^{11} \text{ cm}^{-2}$ were observed in the Si QW with -0.9% tensile strain. However, the increase of strain up to -1.08% resulted in the decline of 2DEG drift mobility down to $2670 \text{ cm}^2 \text{ V}^{-1} \text{ s}^{-1}$ and the pronounced increase of carrier density up to $4.4 \times 10^{11} \text{ cm}^{-2}$. Nevertheless, the pronounced enhancement of 2DEG conductivity was observed.

© 2008 The Japan Society of Applied Physics

DOI: 10.1143/APEX.1.021402

The SiGe heterostructures allow both bandgap and strain engineering based on silicon technology. The modulation doped (MOD) SiGe heterostructures with a tensilely strained Si quantum well (QW) grown on underlying Si(001) or SOI(001) substrates via implementation of an intermediate relaxed SiGe buffer attract much attention for fundamental research and device applications mainly due to high two-dimensional electron gas (2DEG) mobility.¹⁾ The strain narrows the band gap of Si and causes the appearance of QW in the conduction band. Electrons confined in the strained Si QW have lower effective mass that increases their mobility. The reduction of carrier scattering factors such as the inter-valley scattering also leads to enhancement of mobility in this material system. The modulation doping that significantly reduces the ionized background impurity scattering, low threading dislocations density in the relaxed SiGe buffer and low Si QW interface roughness are well known factors that contribute to the enhancement of 2DEG mobility at low-temperatures. Up to date very high low-temperature 2DEG mobilities in the range from $520000 \text{ cm}^2 \text{ V}^{-1} \text{ s}^{-1}$ (at 0.35 K) up to $800000 \text{ cm}^2 \text{ V}^{-1} \text{ s}^{-1}$ (at 15 K) with carrier densities of 7×10^{11} and $2 \times 10^9 \text{ cm}^{-2}$, respectively, are obtained.^{2,3)} These values significantly exceed the mobility of electrons in bulk Si. At room temperature (RT), which is more important for field-effect transistor (FET) device applications, the dramatic progress in enhancement of 2DEG mobility was achieved as well. Drift mobilities in the range from $2600 \text{ cm}^2 \text{ V}^{-1} \text{ s}^{-1}$ (with density of $2 \times 10^{11} \text{ cm}^{-2}$) up to $2830 \text{ cm}^2 \text{ V}^{-1} \text{ s}^{-1}$ (carrier density is not published) were reported so far.^{4,5)} The Hall mobility and sheet carrier density of the samples are typically measured by a combination of resistivity and Hall effect measurements. In the absence of parallel conduction, which is realized in most cases at low-temperatures, the measured Hall mobility and carrier density corresponds to the drift mobility of 2DEG in a Si QW, through appropriate correction with the Hall factor. However, at higher temperatures, particularly at RT, the conventional resistivity and Hall effect measurements yield only an averaged density and mobility of carriers existing not only in the QW layer but also in other parallel conducting ones, such as, the doped layer, the buffer layer, the substrate, and their interfaces. In order to separately find out the transport properties of various carriers existing in multilayer semiconductor heterostructures, the technique of mobility spectrum analysis

(MSA), where the magnetic-field dependencies of magnetoresistance and Hall resistance are measured and analyzed, has to be applied.⁶⁾ In the past, the MSA was used to obtain high RT 2DEG drift mobility of $2700 \text{ cm}^2 \text{ V}^{-1} \text{ s}^{-1}$ with carrier density of $1.7 \times 10^{11} \text{ cm}^{-2}$ in the 20 nm Si QW.⁷⁾ However, aforementioned values of RT 2DEG mobility as well as the most of published data were obtained by simple calculations assuming some number of parallel conduction layers with certain properties in MOD SiGe heterostructures.^{4,5)} This approach can give reasonable results but they are not generally accurate. Probably due to this, there are only few publications where values of RT 2DEG carrier density and mobility are reported together. This makes it quite difficult to compare new results with the published data, because the 2DEG mobility as well as three-dimensional (3D) electron mobility in the bulk strongly depends on the carrier density.

In this paper, we report on RT drift mobility, carrier density and conductivity of the 2DEG confined in 15 nm Si QW, with various tensile strain, of *n*-type MOD Si/Si_{1-y}Ge_y/Si/Si_{1-y}Ge_{1-y}/Si(001) heterostructures. The data were obtained by the maximum-entropy mobility spectrum analysis (ME-MSA)⁶⁾ to clarify the dependence of 2DEG drift mobility on carrier density. The design of samples was chosen to be very similar to those in which high RT 2DEG drift mobility was obtained so far, but their structural properties were tried to be improved.

The *n*-type MOD Si/Si_{1-y}Ge_y/Si/Si_{1-y}Ge_{1-y}/Si(001) heterostructures were grown by combination of gas source molecular beam epitaxy (GS-MBE) and solid source molecular beam epitaxy (SS-MBE) techniques. Their schematic design is shown in Fig. 1. The samples consist of relaxed Si_{1-y}Ge_y buffer necessary to produce tensilely strained Si QWs on underlying Si(001) substrate and MOD region. The Si_{1-y}Ge_y relaxed buffer was grown by GS-MBE at 700 °C on Si(001) substrate. It consists of 1 μm SiGe layer with graded Ge content and 1 μm SiGe layer with uniform Ge content. After the growth, the substrates were removed from the GS-MBE chamber and planarized by chemical mechanical polishing (CMP) in order to produce smooth surface and to minimize the effect of Si_{1-y}Ge_y/Si(001) virtual substrate (VS) surface roughness on mobility of electrons in the Si QW. The cleaned samples were again loaded in the GS-MBE system for the following growth of Si QW region of MOD structures. It consist of 100 nm Si_{1-y}Ge_y buffer, a

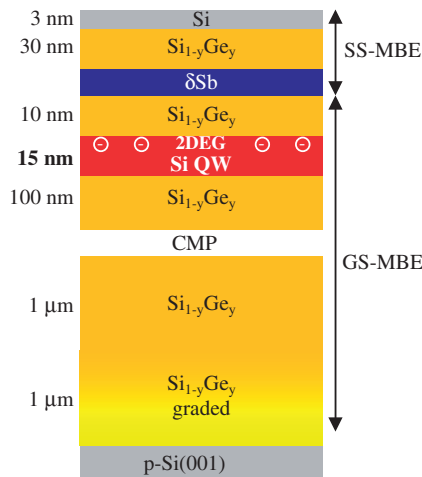


Fig. 1. Schematic designs of *n*-type MOD Si/Si_{1-y}Ge_y/Si/Si_{1-y}Ge_y/Si(001) heterostructures grown by combination of GS-MBE and SS-MBE.

15 nm undoped tensilely strained Si QW layer for 2DEG, and 10 nm Si_{1-y}Ge_y undoped spacer layer. All epilayers were grown at 700 °C in order to obtain Si QW layer of high crystal quality. At this point, the growth was interrupted and wafers were transferred to SS-MBE system where the MOD layers were grown. They consist of a δ -doped Sb layer, a 30 nm Si_{1-y}Ge_y undoped cap layer and 3 nm Si cap layer on the surface. The two samples with Ge content of 0.25 and 0.3 in Si_{1-y}Ge_y layers and consequently -0.9 and -1.08% mismatch tensile strain (as was determined later by structural characterization) in the Si QW layer were grown. Since higher strain allows confinement of more carriers in the Si QW, the Sb doping level was increased from $\sim 1 \times 10^{12}$ up to $\sim 3 \times 10^{12} \text{ cm}^{-2}$ in the sample with higher strain Si QW.

The degree of strain and Ge content in various layers of grown samples were determined with the help of symmetric (004) and asymmetric (224) high-resolution X-ray diffraction (HR-XRD) reciprocal space mapping and micro-Raman spectroscopy measurements at RT. The Si QW layers in all samples were found to be fully strained while the Si_{1-y}Ge_y buffer layers were almost fully relaxed. The desired surface flatness of the grown samples was confirmed by atomic force microscopy (AFM) measurements. The measurements were carried out on several $100 \times 100 \mu\text{m}^2$ surface areas. The average root mean square (RMS) surface roughness of Si_{1-y}Ge_y buffers after CMP was found to be below 1 nm while the further growth of Si QW MOD epilayers caused an increase of it and reappearance of cross-hatch pattern on the surface.

Samples for RT magnetotransport measurements were fabricated in mesa-etched Hall-bar device geometry with the distance of 500 μm between potential contacts and channel width of 100 μm . Ohmic contacts were formed by ion implantation of phosphorous at dose of $1 \times 10^{15} \text{ cm}^{-2}$ and energy 35 keV followed by dopants activation at 700 °C in N₂ ambient for 30 min and final aluminum metallization. The Hall mobility and sheet carrier density of the grown samples were obtained by a combination of resistivity and Hall effect measurements. And the 2DEG drift mobility and carrier density in the Si QW were obtained by ME-

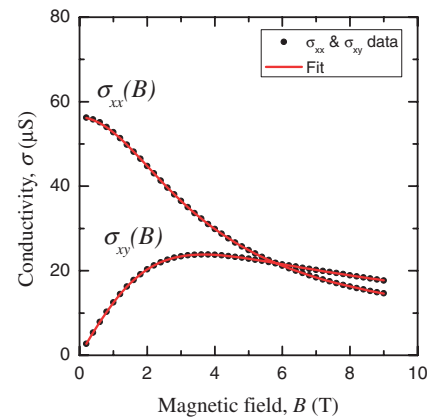


Fig. 2. Measured (circles) at temperature of 290 K and fitted (lines) magnetic field dependence of magnetoconductivity tensor components $\sigma_{xx}(B)$ and $\sigma_{xy}(B)$ of *n*-type MOD Si/Si_{0.75}Ge_{0.25}/Si/Si_{0.75}Ge_{0.25}/Si(001) heterostructure.

MSA where the magnetoresistance and Hall resistance were measured as the magnetic field was swept. The measured data were converted into conductivity tensor components $\sigma_{xx}(B)$ and $\sigma_{xy}(B)$ followed by the ME-MSA fit procedure.⁶⁾ It is worth pointing out that the ME-MSA approach does not require any preliminary assumptions about the number of different types of carriers, and this aspect is very important for transport phenomenon analysis of semiconductor structures.

Figure 2 shows conductivity measured at 290 K and the fitted magnetic field dependence of conductivity tensor components $\sigma_{xx}(B)$ and $\sigma_{xy}(B)$ of *n*-type MOD Si/Si_{0.75}Ge_{0.25}/Si/Si_{0.75}Ge_{0.25}/Si(001) heterostructure. Fitting is seen to be in excellent agreement with the measured data. From this fitting procedure the mobility spectrum shown in Fig. 3 was deduced and it is seen that it consists of three clearly resolved peaks. The strongest peak with the highest negative mobility in the spectrum is attributed to the 2DEG confined in the strained Si QW. The drift mobility, carrier density, and conductivity of the 2DEG extracted from the mobility spectrum are $2900 \text{ cm}^2 \text{ V}^{-1} \text{ s}^{-1}$, $1 \times 10^{11} \text{ cm}^{-2}$, and $45 \mu\text{S}$, respectively. The lower intensity peak with negative mobility well below $1000 \text{ cm}^2 \text{ V}^{-1} \text{ s}^{-1}$ and conductivity of $9 \mu\text{S}$ is attributed to the group of carriers in the Sb doped layer. And the lowest intensity peak with positive mobility and conductivity of just $1.9 \mu\text{S}$ is thought to correspond to the holes in the *p*-type Si substrate. The latter two groups of carriers are from unwanted but existing parallel conduction layers. In contrast to the mobility of carriers in the parallel conducting layers, the 2DEG mobility was found to increase with decreasing temperature and coincide with the Hall mobility at low-temperatures when carriers in parallel conducting layers freeze out. The contribution to the total conductivity of this sample from 2DEG and parallel conduction carriers are 80.5 and 19.5%, respectively. Due to this, the measured Hall mobility of $2390 \text{ cm}^2 \text{ V}^{-1} \text{ s}^{-1}$ (at carrier density of $1.47 \times 10^{11} \text{ cm}^{-2}$) that is shown as a blue line in Fig. 3 is very high and close to the 2DEG drift mobility. It is shown in Fig. 3 for clarity. For the second *n*-type MOD Si/Si_{0.7}Ge_{0.3}/Si/Si_{0.7}Ge_{0.3}/Si(001) heterostructure with higher tensile strain in the Si QW and higher

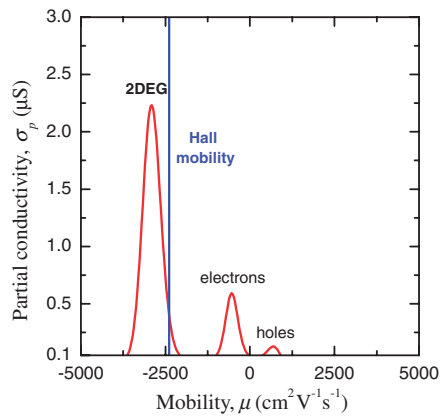


Fig. 3. Mobility spectrum of n-type MOD Si/Si_{0.75}Ge_{0.25}/Si/Si_{0.75}Ge_{0.25}/Si(001) heterostructure as the result of $\sigma_{xx}(B)$ and $\sigma_{xy}(B)$ fit shown in Fig. 2. Hall mobility of the sample is shown for clarity.

level of doping, the Hall mobility of $1360 \text{ cm}^2 \text{ V}^{-1} \text{ s}^{-1}$ (at carrier density of $18.3 \times 10^{11} \text{ cm}^{-2}$) was found. In contrast to the previous sample, the strongest peak in the mobility spectrum is associated with the carriers in parallel conduction. They are electrons with much higher conductivity of $209 \mu\text{S}$. Similar to the first sample, the peak with the highest negative mobility in the spectrum is attributed to the 2DEG confined in the strained Si QW. The drift mobility, carrier density, and conductivity of the 2DEG extracted from the mobility spectrum are $2670 \text{ cm}^2 \text{ V}^{-1} \text{ s}^{-1}$, $4.41 \times 10^{11} \text{ cm}^{-2}$, and $188.6 \mu\text{S}$, respectively. Higher 2DEG carrier density is attributed to higher tensile strain in Si QW layer that results in higher conduction band offset (by around 30 meV) of QW and consequently better electrons confinement. In this sample, 52.6% of total conductivity is concluded to be due to parallel conduction, implying that not all carriers from the MOD supply layer are transferred to the Si QW. Higher level of doping should be also noted to result in the stronger influence of remote ionized impurity scattering on 2DEG, which is one of the reasons of observed degradation of 2DEG drift mobility. Another one is the interface roughness scattering. Because higher carrier density causes 2DEG wave function to move more closer to Si QW and Si_{1-y}Ge_y spacer interface and experience more scattering. Nevertheless, over 4 times enhancement of 2DEG conductivity in the Si QW with higher tensile strain is obtained even in this sample in spite of around 8% decline of the drift mobility.

Figure 4 shows two-dimensional (2D) drift mobility dependence on 2D carrier density at RT. The highest values for previously published 2DEG drift mobilities in the 10 nm and 20 nm strained Si QWs are shown along with the results obtained in this work.^{5,7} The highest 2DEG mobility of $2830 \text{ cm}^2 \text{ V}^{-1} \text{ s}^{-1}$ reported so far is not shown in this figure because the carrier density was not published.⁴ It is clearly seen that the drift mobility of $2900 \text{ cm}^2 \text{ V}^{-1} \text{ s}^{-1}$ obtained in this work is the highest among 2DEG. It is also interesting to note the similar trend of the decrease of mobility with the increase of carrier density. However, it is also seen in this figure that the drift mobility of $3100 \text{ cm}^2 \text{ V}^{-1} \text{ s}^{-1}$ at carrier density of $4.1 \times 10^{12} \text{ cm}^{-2}$ is obtained for 2DHG confined in the compressively strained 20 nm Ge QW grown on

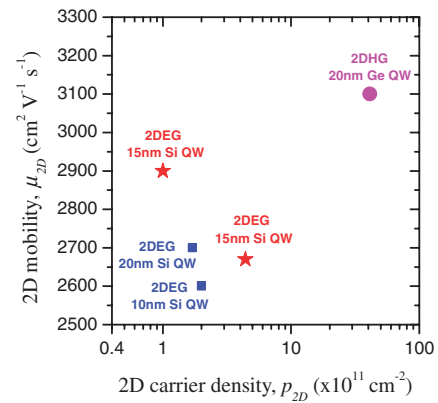


Fig. 4. The 2D drift mobility as a function of density at room-temperature. The 2DEG with the highest reported so far mobilities in 10 and 20 nm Si QWs are shown by squares.^{5,7} The 2DEG in 15 nm Si QWs with various state of strain obtained in this work are shown by stars. The 2DHG with the highest drift mobility in a 20 nm Ge QW from is shown by circle.⁸

Si_{0.45}Ge_{0.55}/Si(001) VS.⁸ This the highest 2DHG drift mobility obtained in the strained Ge QW exceeds not only 2DEG ones obtained in the strained Si QWs but also hole and electron mobilities in bulk Si and Ge at RT, even though the carrier density is extremely high.

In summary, the transport properties of 2DEG confined in the tensile strained 15 nm Si QW of n-type MOD Si/Si_{1-y}Ge_y/Si/Si_{1-y}Ge_{1-y}/Si(001) heterostructures were obtained by mobility spectrum analysis at RT. The highest 2DEG drift mobility of $2900 \text{ cm}^2 \text{ V}^{-1} \text{ s}^{-1}$, which is the highest RT 2DEG drift mobility reported so far, was obtained in the sample with -0.9% tensile strain 15 nm Si QW and with low doping. Higher strain of -1.08% and modulation doping was, however, found to cause enhancement of 2DEG carrier density but decline of mobility. Nevertheless, over 4 times enhancement of 2DEG conductivity was observed, which is important for application of this material system to the high performance FET devices.

Acknowledgement This work was supported by “High-Tech Research Center” Project for Private Universities: matching fund subsidy from the Ministry of Education, Culture, Sports, Science and Technology (MEXT) 2003–2008, the Japan Society for the Promotion of Science (JSPS) funding for young researchers No. 18760019, in part by a Grant-in-Aid for Scientific Research by MEXT, Specially Promoted Research No. 18001002 and in part by Special Coordination Funds for Promoting Science and Technology.

- 1) F. Schaffler: *Semicond. Sci. Technol.* **12** (1997) 1515.
- 2) K. Ismail, M. Arafa, K. L. Saenger, J. O. Chu, and B. S. Meyerson: *Appl. Phys. Lett.* **66** (1995) 1077.
- 3) N. Sugii, K. Nakagawa, Y. Kimura, S. Yamaguchi, and M. Miyao: *Semicond. Sci. Technol.* **13** (1998) A140.
- 4) K. Ismail, S. F. Nelson, J. O. Chu, and B. S. Meyerson: *Appl. Phys. Lett.* **63** (1993) 660.
- 5) S. F. Nelson, K. Ismail, J. O. Chu, and B. S. Meyerson: *Appl. Phys. Lett.* **63** (1993) 367.
- 6) S. Kiatgamolchai, M. Myronov, O. A. Mironov, V. G. Kantsler, E. H. C. Parker, and T. E. Whall: *Phys. Rev. E* **66** (2002) 036705.
- 7) G. Hock, M. Gluck, T. Hackbarth, H. J. Herzog, and E. Kohn: *Thin Solid Films* **336** (1998) 141.
- 8) M. Myronov, K. Sawano, Y. Shiraki, T. Mouri, and K. M. Itoh: *Appl. Phys. Lett.* **91** (2007) 082108.